Proceedings of the 32nd ISR(International Symposium on Robotics), 19-21 April 2001

Goal-Directed Navigation of an Autonomous Flying Robot Using Biologically Inspired Cheap Vision

Fumiya Iida
AI Lab, Department of Information Technology, University of Zurich
Winterthurerstr. 190, CH-8057 Zurich, Switzerland
E-mail : iida@ifi.unizh.ch

Abstract

In nature, flying insects are capable of surprisingly good navigation, despite the small size and relative simplicity of their brains. Recent experimental research in biology has uncovered a number of different ways in which insects use cues derived from optical flow for navigational purposes, such as obstacle avoidance, safe landing and dead-reckoning. Inspired by the visual navigation of flying insects, this paper presents a model of vision-based navigation using Elementary Motion Detectors (EMDs). The performance tests with an autonomous flying robot successfully demonstrate goal-directed navigation in an unstructured environment, as well as obstacle avoidance and course stabilization behaviors. Further investigation in the simulation shows that goal-directed navigation can be potentially achieved by simple visual processing, and that the design flexibility of this approach leads to high adaptivity to the given task-environment.

1. Introduction

In nature, flying insects navigate through a complex environment in a robust manner, despite their tiny brains. Behavioral studies with insects have revealed that a number of important navigational abilities rely mainly on visual information: more specifically, image motion induced by ego-motion plays a crucial role in their navigation. However, vision is generally regarded as a computationally intensive task, thus powerful hardware is required to operate in real time. From an algorithmic viewpoint, the structure of visual scenes is often very complex, and it can be difficult to extract relevant information robustly. Especially, the traditional technique of optical flow requires feature tracking, which is possible only if visible objects possess distinguishing features identified consistently in image sequences[1]. Therefore, due to the limited weight constraint and potentially hazardous conditions, flying artifacts rely heavily on other sensory devices, such as GPSs, gyroscopes, compasses, ultrasonic sensors, inclinometers, accelerometers, and laser rangefinders[2, 3, 4].

Recently, navigation using biologically inspired optical flow has been investigated mainly on land-based agents. The basic behaviors observed in flying insects, i.e. obstacle avoidance, fixation behaviors and so on, were demonstrated with relatively simple mechanisms[5, 6, 7]. Owing to its simplicity, such mechanisms have been incorporated in a robot exclusively using analog hardware[5]; a VLSI implementation has been also realized[8]. In a similar way, simulated flying agents were used for altitude control and obstacle avoidance[9, 10, 11], and a robotic gantry demonstrated the landing behavior of flies[12].

In our previous work, a biologically inspired model of goal-directed navigation was tested with a freely flying robot[13]. One of the interesting properties of this approach is the lower computational cost and the design flexibility that leads to the adaptivity to the given task-environment. In this paper, we conduct further analysis with additional experiments using the flying robot, as well as simulation studies.

In the following section, we introduce navigation mechanisms of flying insects. We then propose a goal-directed navigation method in section 3, and show the experiments with an autonomous flying robot in section 4. Further analysis with simulation is discussed in section 5.

2. Navigation in flying insects

The vision systems of flying insects are exquisitely sensitive to motion, because visual motion induced by ego-motion can tell the animal much about its own motion and also about the structure of its environment. Behavior experiments with flies and bees show a number of different ways in which insects use cues derived from optical flow for navigational purposes (for review, see [14]). Early studies showed that a tethered fly inside a striped drum tends to turn in the direction in which the drum is rotated[15]. This reaction, so-called optomotor response, serves to help the insect maintain a straight course by compensating for undesired deviations. For speed control, honeybees have been shown to regulate flight speed by monitoring the speed of apparent motion[16]. For example, when forced to fly down a tapered tunnel, bees slow down as they approach the narrowest section and speed up again as the tunnel widens once more. A similar mechanism can be used for achieving a smooth landing[12]. By holding the angular velocity of the image of the surface constant as insects approach the ground, the forward and descent speeds are automatically reduced as the surface is approached and are both close to zero at touch down. For long distance navigation, recent studies of bees' behavior suggested that the amount of image motion plays an important role in estimating the distance traveled[17].

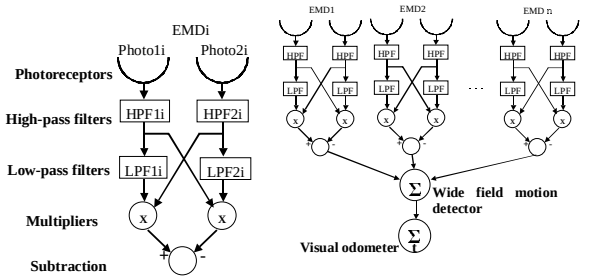

Figure 1. **Left:** The Reichardt model of EMD. **Right:** The visual odometer based on a wide field motion detector.

On the basis of above mentioned behavioral experiments as well as electrophysiological studies, a model of motion detection in the insect's nervous system, the Elementary Motion Detector (EMD), has been proposed (for review, see [18]). A well-known model of the EMD is the so-called Reichardt detector, which belongs to a class of correlation-type detectors, shown in Figure 1. Two adjacent photoreceptors send their outputs to temporal high-pass filters which remove constant illumination containing no motion information. These signals are then "delayed" by exploiting the phase lag inherent in a first order temporal low-pass filter. While not a true time delay, the low-pass filter is a good approximation that biology appears to use. Delayed channels are then correlated with adjacent, non-delayed channels by means of a multiplication operation. Finally the outputs of two opponent EMDs are subtracted to yield a strongly direction-sensitive response.

Although the nature of the neural mechanisms and the location in the visual pathway remains to be elucidated, some behaviors of the motion sensitive neurons in insects can be well characterized by this motion detector model[14]. The salient properties of the movement-sensitive mechanism underlying these responses are that it is directional, and it does not encode the speed of the moving image. Rather, it is sensitive to the temporal frequency of intensity fluctuations generated by the moving image, and therefore confounds the speed of the image with its spatial structure.

3. Navigation of a flying robot using the Elementary Motion Detectors

In the rest of this paper, we focus on goal-directed navigation by using EMDs. The navigation mechanism used in this paper is built on the basis of two evidences gained in behavior studies of insects. Firstly, a biologically inspired visual odometer is applied for the distance measurement, since bees are known to gauge the distance in terms of the amount of image motion. In this method, the distance from an initial location to a destination can be estimated by accumulating responses of EMDs over time. However such a visual odometer would work accurately only if the agent were to follow a fixed route each time, because the total amount of image motion that is experienced during the trip would depend on the distances to the various objects that are passed during navigation. Secondly, therefore, we assume that sensory motor coordination, which regulates the courses

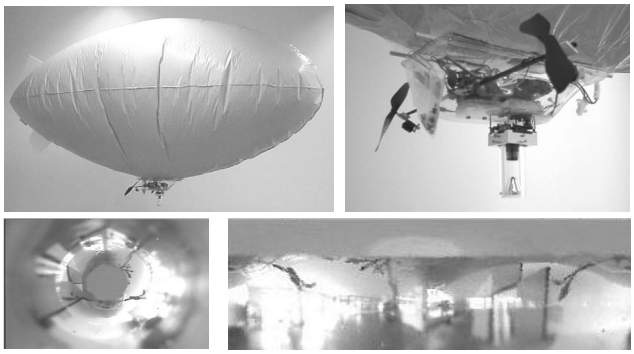

Figure 2. **Top:** The autonomous flying robot, *Melissa*, and its gondola. **Bottom:** An image obtained by the panoramic vision system and its log-polar transformed image, which is also used in the experiments.

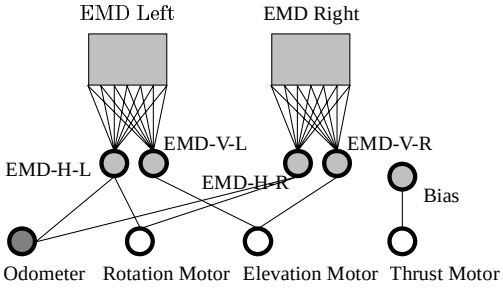

Figure 3. The sensory-motor control circuit.

the robot follows, would play an important role in the context of goal-directed navigation. This reaction is also observed in behaviors of flying insects[19].

To test this mechanism, we developed an autonomous flying robot, shown in Figure 2. The flying robot *Melissa* is a blimp-like flying robot, which consists of a helium balloon, a gondola hosting the onboard electronics, and a host computer. The balloon is 2.3m long and has a lift capacity of approximately 400g. Inside the gondola, there are 3 motors for rotation, elevation and thrust control, a four-channel radio link, a miniature panoramic vision system, and the batteries. The panoramic mirror was developed based on a panoramic optics study[20] and has a hyperbolic surface that provides a visual field of 360 degrees on the horizontal plane and 260 degrees vertically. The control process of *Melissa* can be decomposed to three basic steps. First, the video signal from the CCD camera attached to the gondola is transmitted to the host computer via a wireless video link. Second, the images are then digitized on the host computer, which also performs the image processing in order to determine the target motor command. And third, the motor command is sent to the gondola also via radio transmission.

The control architecture of the robot is shown in Figure 3. The left and right visual fields consist of two dimensional arrays of EMDs, in which EMDs are oriented both horizontally and vertically to measure both movements[18]. The number of EMDs in each array can be highly flexible; in the extreme case, one EMD on each side and another for

vertical one is sufficient (therefore, only 5 pixels are required for 3-D control). In addition, parameters of the EMDs, such as low-pass filter constants, can be set independently, but only homogeneous distributions are employed in this paper. The responses from both horizontal and vertical wide field EMDs are extracted, and provide inputs to the visual odometer as well as to a sensory-motor circuit. In the visual odometer neuron, the given inputs from the horizontal EMDs (EMD_H_R and L in Figure 3) are accumulated over time. In the sensory-motor circuit, the right and left horizontal EMDs are connected to the rotation motor neuron. The right and left vertical EMD neurons (EMD_V_R and L) are connected to the elevation motor neuron, whereas the connection weights are chosen in such a way to suppress vertical motion, i.e. to retain height. The thrust motor neuron is connected to a bias neuron that drives the robot forward at a constant speed. The connection weights are set by hand, and are not changed during the experiments.

4. Experiment with a freely flying robot

4.1. Course stabilization behavior

To evaluate the performance, we conducted a set of experiments in an uncontrolled indoor environment. Figure 4 shows the experimental setup. We used two video cameras to track and record the absolute trajectory of the robot for later analysis. In this experiment, the connection weights between the horizontal EMDs (EMD_H_R and L) and the rotation motor neuron were hand-tuned in such a way that a small difference between the EMD_H_R and EMD_H_L activations is maintained. This scheme corresponds to a course stabilization behavior, in which the robot follows a "straight route". The 80 x 80 pixels (40 x 40 EMDs) on each left and right lateral views in the panoramic image were used as inputs to the photoreceptors. All experiments were conducted with the same initial conditions, i.e. initial position, initial orientation, and connection weights. In this experiment, the robot performed the control procedure for 20 seconds; the procedure was repeated 5 times.

In the upper graphs of Figure 5, the plots show 3-D coordinates of the robot in one-second steps. Since the robot has the same neural connections through all of the 5 trials, the trajectories of the robot are similar. Figure 5 also shows the visual odometer responses that the robot obtains during each trial. Since the robot follows similar routes, the visual odometer measures almost the same distances even with natural stimuli in the office environment. In summary, considering that the robot follows the same route, and it measures the same "distance" robustly, this mechanism could be used for navigating between different places in the environment, i.e. for goal-directed navigation.

4.2. Obstacle avoidance behavior

In the next experiment, the low-pass filter parameters and the number of EMDs were hand-tuned specifically for obstacle avoidance in which, when the right EMDs have higher activation, i.e. high speed image motion, the rotation motor neuron will react to turn left, and vise versa. This

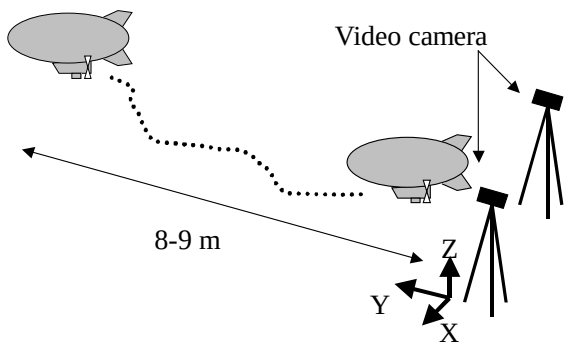

Figure 4. The experimental setup

mechanism will make the robot follow a route away from walls and obstacles, because image motion is faster when the robot comes closer to objects. In this experiment, we used 100 x 80 pixels (50 x 40 EMDs) on each lateral view; the robot performed the control for 25 seconds; the trial was repeated 5 times. The other parameters and experimental setup were the same as the previous experiment.

Figure 6 shows the trajectories and the visual odometer responses. As shown in the upper graphs, the robot reacted to the wall on its left side (which is not shown in the graph), and turned away to its right in all of the trials. The visual odometer responses also estimated the distance correctly.

4.3. Discussion

The way a flying robot achieves goal-directed navigation in these experiments is apparently different from those of traditional map based approaches. There is no explicit map in the robot brain, rather the navigation is dependent on the interaction between the entire robot and environment. For example, sensor morphology plays an important role in this scheme, since the visual odometer can work precisely only when sensors can sense the lateral image motion. (The frontal part of the image does not move much, when the robot goes straight.) However, if sensors were positioned only on a part of the lateral view, obstacle avoidance would not be performed well, because the robot could not see obstacles approaching. Another important point is parameters in the EMDs and the sensory-motor connections. As described earlier, EMD arrays are sensitive to a particular spatio-temporal frequency, thus the parameters, such as time-delay constants in low-pass filters, determine the output activation, which leads to the robot behaviors together with the sensory motor connection weights. It is not clearly shown in these experiments, but the properties induced by the physical body of the robot, such as inertia, air-friction, motor torque, etc. might be important as well. For example, if the robot could move or turn faster than a peak image frequency of EMDs, the sensory-motor loop would become unstable. This reaction has been reported in physiology study of flies[21].

An advantage of this approach is that neither computationally intensive feature tracking for optical flow nor precise calibration is required even in an uncontrolled

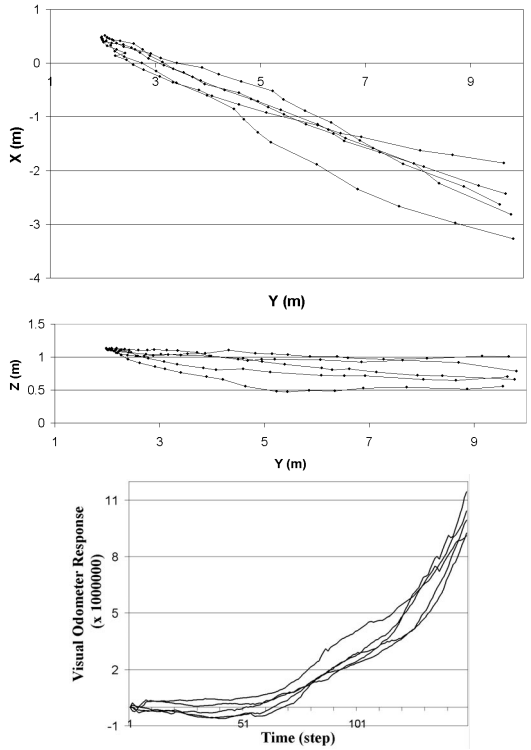

Figure 5. **Top and Middle:** 3-D trajectories of the flying robot during the course stabilization experiments. **Bottom:** Visual odometer responses.

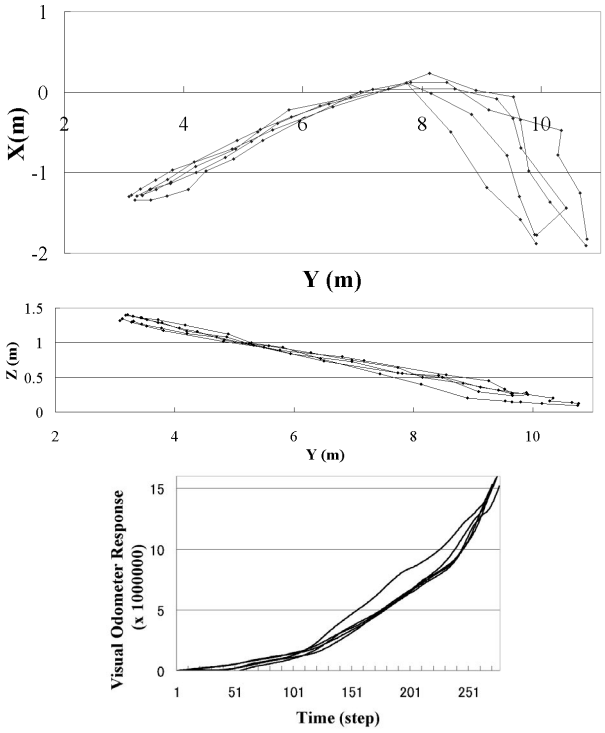

Figure 6. **Top and Middle:** 3-D trajectories of the flying robot during the obstacle avoidance experiments. **Bottom:** Visual odometer responses.

environment. As long as images contain intensity fluctuations, this navigation mechanism performs goal-directed navigation. Another advantage is that it is relatively easy to change the behavior without changing the basic mechanisms. In these experiments, for example, the course stabilization and obstacle avoidance behaviors were demonstrated by simply changing the low-pass filter parameters and the number of EMDs, however it is also intuitive that other important behaviors for flying insects could be potentially achieved with similar mechanisms.

5. Simulation Experiments

5.1. Method

This section presents a simple simulation experiment to investigate the influence of parameters on the proposed approach. For the sake of convenience, we conducted the simulations in a 2-D environment. As shown in Figure 7, an agent navigates through a corridor, both sides of which have walls with one-dimensional sinusoidal intensity patterns. The same controller described in section 2 is implemented on the agent, but it has no inertia or friction, thus the position and the orientation of the agent are simply calculated from visual inputs in the previous step. The agent starts to navigate from the same initial condition and continues until it hits the walls or reaches the end of the experimented area.

We tested 2, 40, and 90 pixels on each lateral view of the agent (therefore the agent has 2, 40, and 90 EMDs in total respectively), each of them are positioned at a constant

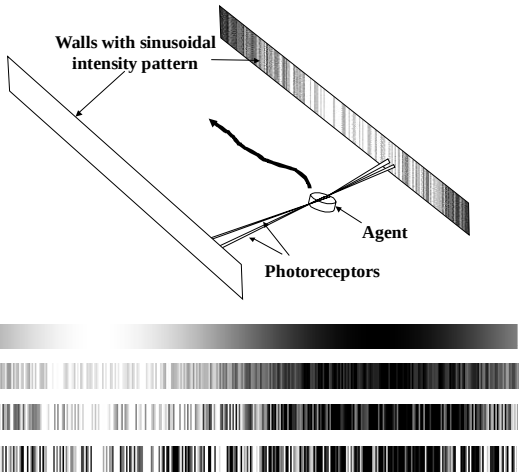

Figure 7. Top: The simulation setup. **Bottom:** The typical patterns used on the wall. (Noise 0, 20, 50 and 100 % from top to bottom.)

angular distance of 2 degrees. We began with a simple environment in which walls in the corridor contains sinusoidal intensity patterns. Noise was then added by means of the following equation.

$$\mathbf{I}(\mathbf{x}) = 128 + 256 \times \sin(\mathbf{x}) + 256 \times \mathbf{Noise\_Level} \times \mathbf{Random} \quad (1)$$

where $\mathbf{I}(\mathbf{x})$ is the intensity at location $\mathbf{x}$, and **Random** is a random value between 0 and 1. We tried **Noise_Level** values

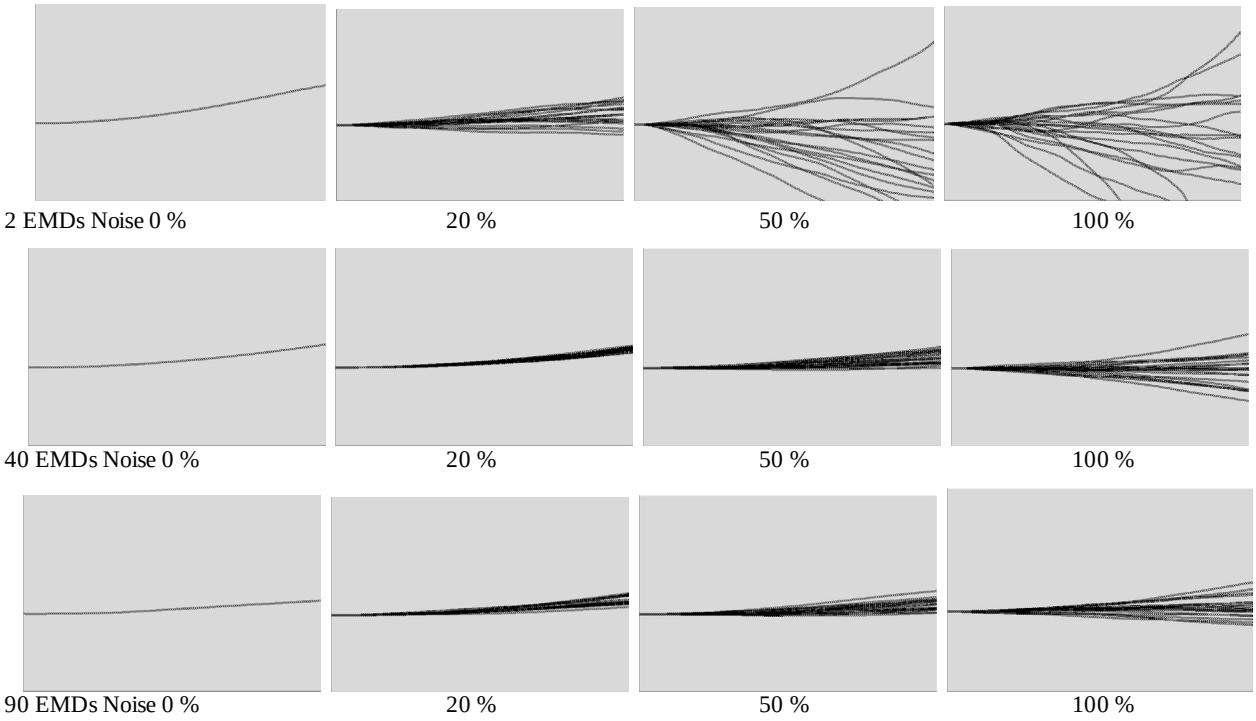

Figure 8. Trajectories of the simulated agent. Each graph contains the results from 20 trials with different wall patterns.

of 0, 20, 50, and 100 %. This noise corresponds to a variation of spatial structure in the real environment. Figure 7 shows the typical sinusoidal patterns at each noise level. With each combination of the number of EMDs and the noise level, 20 trials were tested using the different wall patterns generated by different random seeds.

5.2. Result and discussion

Figure 8 illustrates the trajectories from each trial, and Figure 9 shows the mean visual odometer responses of 20 trials and the standard deviations (SD) as percentage of the mean visual odometer responses. In case of **Noise_Level** 0%, the proposed method can achieve goal-directed navigation with only 2 EMDs (4 pixels); the agent follows the same route and measures the distance correctly, i.e. zero SD. In the noisy conditions, however, the trajectories spread out in earlier stages of the navigation, which lead to larger odometer errors. In the cases of 40 and 90 EMDs, on the other hand, deviations of routes are relatively small. These results suggest that the larger numbers of EMDs improve the performance in the noisy environments, namely goal-directed navigation can be achieved robustly even when spatial structures of the environment are modified. This also implies the design flexibility of the proposed approach in a sense that designers (or an evolutionary process) can flexibly change the architecture of the agent to adapt to the complexity of the given task-environments.

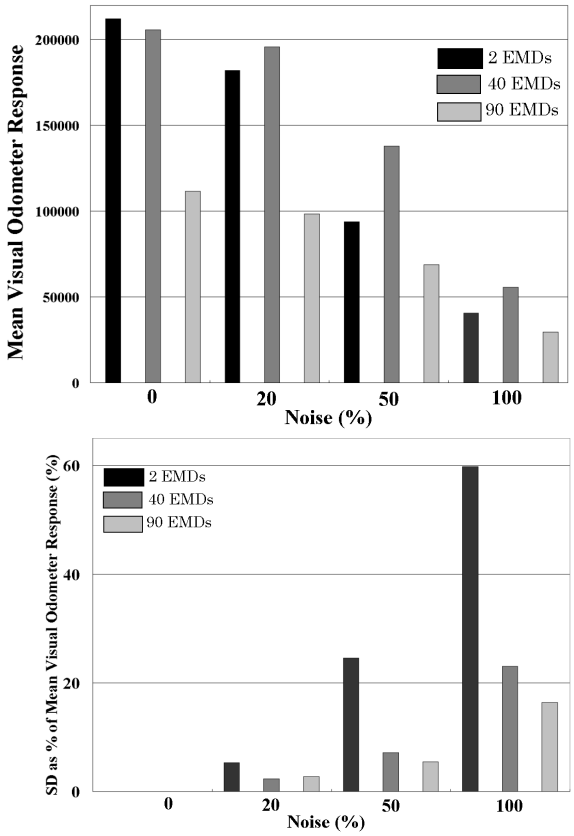

Figure 9. Top: The mean visual odometer responses of 20 trials. **Bottom:** The standard deviations as percentage of the mean visual odometer responses.

6. Conclusion

The concept of “cheap vision” is summarized in [22], and it is largely employed in the proposed scheme of goal-directed navigation. This paper investigated mainly two points; simple image processing and design flexibility, which lead to robust control architecture and adaptivity to the given environment. The control of our blimp-like robotic platform is by far simpler than those of other platforms, such as helicopters. However, by enhancing this “cheap vision” approach, it would be possible to realize more sophisticated controls for more demanding situations with a simpler architecture, as the natural evolution has found a solution for flying insects.

Acknowledgements

I would like to thank Dimitrios Lambrinos and Rolf Pfeifer for valuable discussions and suggestions. This work is supported by the Swiss National Science Foundation, grant no 2000-061372.00, and the Swiss Federal Office for Education and Science (VIRGO TMR network, BBW-No. 96.0148).

References

[1] O. Amidi, T. Kanade, and K. Fujita, "A Visual Odometer for Autonomous Helicopter Fight," Intelligent Autonomous Systems, Y. Kakazu et al. (Eds.), IOS Press, pp.123-130, 1998.

[2] A. H. Fagg, M. A. Lewis, J. F. Montgomery, G. A. Bekey, "The USC Autonomous Flying Vehicle: an Experiment in Real-Time Behavior-Based Control," IEEE/RSJ International Conference on Intelligent Robots and Systems (IROS), Yokohama, Japan, pp. 1173-80, 1993

[3] S. Fürst, E. D. Dickmanns, "A vision based navigation system for autonomous aircraft," Intelligent Autonomous Systems, Y. Kakazu et al. (Eds.), IOS Press, pp.765-774, 1998

[4] J. R. Miller and O. Amidi, "3-D Site Mapping with the CMU Autonomous Helicopter," Intelligent Autonomous Systems, Y. Kakazu et al. (Eds.), IOS Press, pp.765-774, 1998.

[5] N. Franceschini, J. M. Pichon, C. Blanes, “From insect vision to robot vision,” Phil. Trans. R. Soc. Lond. B, 337, pp. 283-294, 1992

[6] S. A. Huber and H. H. Bülthoff, "Modeling Obstacle Avoidance Behavior of Flies Using an Adaptive Autonomous Agent," Proceedings of 7th International Conference on Artificial Neural Networks, ICANN ’97, W.Gerstner et al. (Eds.), pp.709-714, 1997

[7] S. A. Huber, M. O. Franz, H. H. Bülthoff, "On robots and flies: Modeling the visual orientation behavior of flies, " Robotics and Autonomous Systems 29, Elsevier, pp.227-242, 1999.

[8] R. R. Harrison, C. Koch, “A neuromorphic visual motion sensor for real-world robots,” Workshop on Defining the Future of Biomorphic Robotics, IROS'98, 1998

[9] F. Mura, N. Franceschini, “Visual control of altitude and speed in a flying agent,” Proceedings of 3rd international conference on Simulation of Adaptive Behavior: From Animal to Animats III, pp.91-99, 1994

[10] T. Netter, and N. Franceschini, "Towards nap-of-the-earth flight using optical flow, " Proceedings of ECAL99, pp. 334-338, 1999

[11] T. R. Neumann, S. A. Huber, H. H. Bülthoff, "Minimalistic Approach to 3D Obstacle Avoidance Behavior from Simulated Evolution," Proceedings of 7th International Conference on Artificial Neural Networks, ICANN ’97, W.Gerstner et al. (Eds.), pp. 715-720,1997

[12] M. V. Srinivasan, S. W. Zhang, J. S. Chahl, E. Barth, S. Venkatesh, "How honeybees make grazing landings on flat surfaces," Biol. Cybern. 83, pp.171-183, 2000.

[13] F. Iida, D. Lambrinos, “Navigation in an autonomous flying robot by using a biologically inspired visual odometer”, Sensor Fusion and Decentralized Control in Robotic System III, Photonics East, Proceeding of SPIE, vol. 4196, pp.86-97, 2000.

[14] M. V. Srinivasan, M. Poteser, K. Kral, “Motion detection in insect orientation and navigation,” Vision Research 39, pp. 2749-2766, 1999

[15] W. Reichardt, “Movement perception in insects,” In W. Reichardt (Eds.), Processing of optical data by organisms and machines, pp.465-493, New York: Academic, 1969.

[16] M. V. Srinivasan, S. W. Zhang, M. Lehrer, T. S. Collett, “Honeybee navigation en route to the goal: visual flight control and odometry,” In Navigation (ed. R. Wehner, M. Lehrer and W. Harvey). Journal of experimental Biology. 199, pp. 155-162, 1996

[17] M. V. Srinivasan, S. Zhang, M. Altwein, and J. Tautz, “Honeybee Navigation: Nature and Calibration of the "Odometer" ,” Science, vol. **287**, pp. 851-853, 2000.

[18] Borst, A., Egelhaaf, M., “Detecting visual motion: Theory and models, Visual Motion and its Role in the Stabilization of Gaze,” Eds. F.A. Miles and J. Wallman, Elsevier Science, pp. 3-27, 1993

[19] M. V. Srinivasan, S. W. Zhang, and N. Bidwell, “Visually mediated odometry in honeybees,” Journal of Experimental Biology, 200, pp. 2513-2522, 1997

[20] J. S. Chahl, M. V. Srinivasan, “Reflective surfaces for panoramic imaging,” Applied Optics, vol. 36, No. 31, pp. 8275-8285, 1997

[21] A.-K. Warzecha, M. Egelhaaf, “Intrinsic properties of biological motion detectors prevent optomotor control system from getting unstable”, Proc.Roy.Soc.Lond. 351, 1579-1591, 1996

[22] R. Pfeifer, D. Lambrinos, “Cheap Vision - Exploiting Ecological Niche and Morphology”, Theory and practice of informatics: SOFSEM 2000, 27th Conference on Current Trends in Theory and Practice of Informatics, Milovy, Czech Republic; Vaclav Hlavac, Keith G. Jeffery, Jiri Wiedermann [et al.] (Eds.), pp. 202-226, November 25 - December 2, 2000.